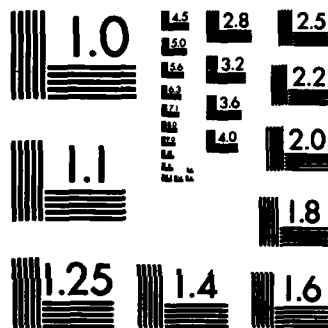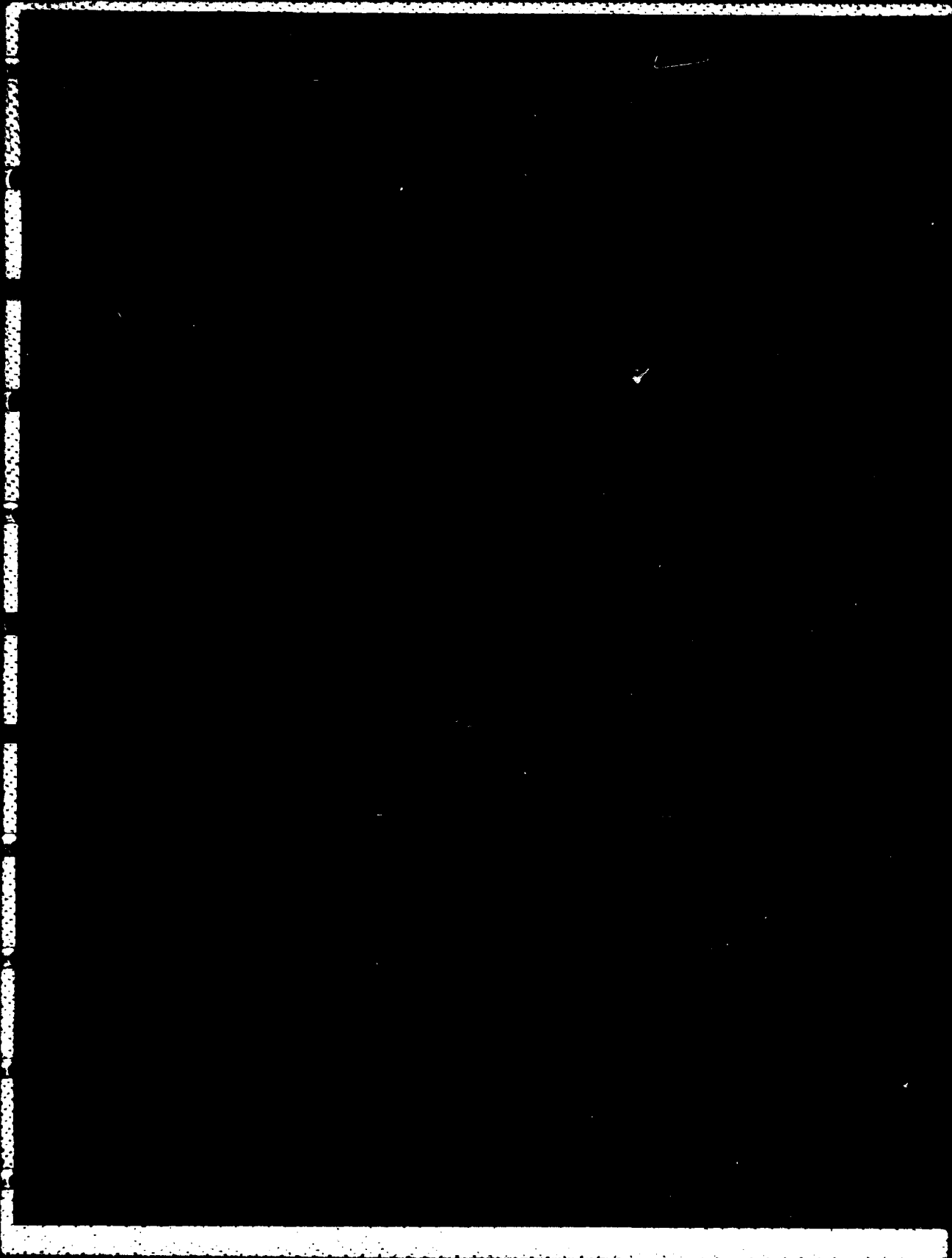END

MICROCOPY RESOLUTION TEST CHART
NATIONAL BUREAU OF STANDARDS-1963-A

Again referring to Fig.2, the total Johnson noise delivered to the amplifier

input terminals is

REPORT DOCUMENTATION PAGE	READ INSTRUCTIONS BEFORE COMPLETING FORM

1. REPORT NUMBER	2. GOVT ACCESSION NO.	3. RECIPIENT'S CATALOG NUMBER
NRL Memorandum Report 5211	AD-A134 139	

4. TITLE (and Subtitle)	5. TYPE OF REPORT & PERIOD COVERED
ANALYSIS OF THE PERFORMANCE OF THE FREE ELECTRON BOLOMETER	Final report on one phase of a continuing NRL problem.
	6. PERFORMING ORG. REPORT NUMBER

7. AUTHOR(s)	8. CONTRACT OR GRANT NUMBER(s)
W.J. Moore, H.S. Newman, and D.C. Webb	

9. PERFORMING ORGANIZATION NAME AND ADDRESS	10. PROGRAM ELEMENT, PROJECT, TASK AREA & WORK UNIT NUMBERS
Naval Research Laboratory Washington, DC 20375	61153N; RR021-01-42; 68-1775-0-3

11. CONTROLLING OFFICE NAME AND ADDRESS	12. REPORT DATE
Office of Naval Research Arlington, VA 22217	November 3, 1983
	13. NUMBER OF PAGES
	33

14. MONITORING AGENCY NAME & ADDRESS(if different from Controlling Office)	15. SECURITY CLASS. (of this report)
	UNCLASSIFIED
	15a. DECLASSIFICATION/DOWNGRADING SCHEDULE

16. DISTRIBUTION STATEMENT (of this Report)

Approved for public release; distribution unlimited.

17. DISTRIBUTION STATEMENT (of the abstract entered in Block 20, if different from Report)

18. SUPPLEMENTARY NOTES

19. KEY WORDS (Continue on reverse side if necessary and identify by block number)

Bolometer
Infrared and millimeter waves
Heterodyne detection
Noise

20. ABSTRACT (Continue on reverse side if necessary and identify by block number)

The free electron bolometer (FEB) can be employed as a rugged, environmentally stable mixer and detector at frequencies above 100 GHz. This record shows how circuitry, material parameters, and operating conditions affect FEB performance. In particular, calculations of the expected noise equivalent power and noise temperature of the device are presented for general bias and IF matching conditions.

DD FORM 1473 1 JAN 73   EDITION OF 1 NOV 65 IS OBSOLETE
S/N 0102-014-6601

CONTENTS

DTIC

S ELECTE D

OCT 2 8 1983

B

Accession For

NTIS ᴄᴘᴀ&I ✓

DTIᴄ ᴛᴀʙ ☐

Unannounced ☐

Justification

By

Distribution/

Availability Codes

Dist	Avail and/or Special
A	

ANALYSIS OF THE PERFORMANCE OF THE FREE ELECTRON BOLOMETER

The free electron bolometer (FEB) has been in use as a far infrared and millimeter-wave detector since the pioneering work of Putley [1] and Kinch and Rollin [2]. Several contributions to the technology and theory of operation of these devices have appeared subsequently. At present, FEBs provide rugged, environmentally stable, high sensitivity devices with superior performance above about 100 GHz. This report shows how circuitry, material parameters and operating conditions affect FEB performance, the overall objective being to realize improved performance at high information rates.

Past studies of InSb FEB performance [3-6] have made one or more simplifying assumptions which limit the application of the models to higher temperatures. In particular, complete calculations of the expected noise equivalent power (NEP) or noise temperature for general bias and IF match conditions and for local oscillator power optimization have not appeared. Thus the purpose of this report is to provide a complete modeling of FEBs in order to allow an accurate determination of the performance available from these devices in rapid response time applications.

1. Device Modeling – Signal Analysis

Modeling of FEB performance will be based on the system shown schematically in Figure 1. The bolometer effect takes place in the free-electron gas at temperature T_e which is loosely coupled to the lattice at temperature T_L through a thermal conductance K. Power from the microwave or infrared radiation and bias circuit is absorbed by the electron gas. The lattice is assumed to be tightly coupled to the heat sink through a large thermal conductance $G_{thermal}$. Energy absorbed by the free-electron gas produces an increase in free electron mobility which varies with temperature as

Radiation

Electron Gas T_e

Thermal
Conductance K

Lattice T_L

Thermal
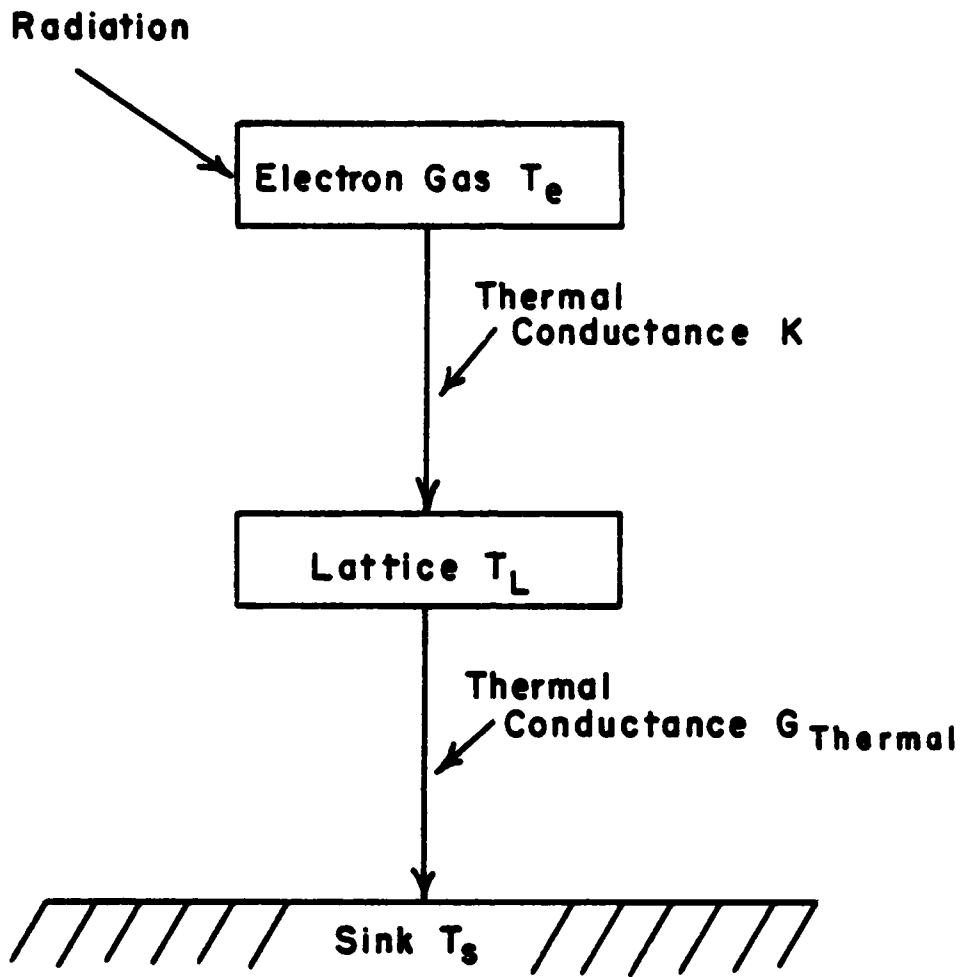Conductance $G_{Thermal}$

Sink T_s

Fig. 1   Schematic representation of the free-electron bolometer.

$$\mu \propto T_e{}^n \qquad (1)$$

When the free electron mobility is limited by ionized impurity scattering
$n \approx 3/2$. Energy is removed from the electron gas by scattering processes
resulting in a decreasing device response time as the lattice temperature, T_L,
is increased. We will use the following definitions in the derivations:

Z_o impedance of free space

T_L lattice temperature

T_o steady state electron gas temperature

T_1 time varying component of electron gas temperature

n normalized derivative of bolometer conductance with temperature

B bandwidth of the bolometer

P_{dc} bias power dissipated in the bolometer

P_{rf} radiation (microwave or rf) incident on the bolometer

A absorption coefficient of bolometer at microwave frequencies

η IR quantum efficiency

P_1 time varying component of incident radiation power

P_{LO} local oscillator power incident on bolometer

P_s signal power incident on bolometer

P_{bg} background noise power

P_o $A_o P_{LO} + P_{dc}$, the total of bias and local oscillator power dissipated
in the bolometer

V_B steady state dc voltage across bolometer

G_L dc bias conductance

G_a amplifier input conductance

G_B bolometer conductance

G_{Bo} steady state value of bolometer conductance

G_{B1} time varying part of bolometer conductance

3

The general approach followed in this section is similar to that of refs. 4 and 5 so will only be sketched briefly here.

The circuit in which the bolometer is assumed to be embedded is shown in Fig. 2. The total power dissipated in the bolometer will be determined by the total of the absorbed radiation and bias power delivered to the bolometer. In general, this can be expressed as:

$$P(t) = P_{dc}(t) + A(t)P_{rf}(t)$$

where A is the absorption coefficient at the frequency of the incident radiation, P_{dc} is the power delivered from the dc bias source, and P_{rf} is the incident (not absorbed) radiation power. The bolometer will not, in general respond directly to an rf frequency but only to an IF frequency. Thus

$$P_{rf}(t) = P_{rfo} + P_{IF} \, e^{i\omega t}$$

where P_{rfo} is the average rf power incident upon the bolometer. The bolometer conductance G_B will also have a time-varying part

$$G_B = G_{Bo} + G_{B1} \, e^{i\omega t}$$

and this in turn will lead to a time variation in the bias power P_{dc} and absorption coefficient. Thus

$$P_{dc}(t) = P_{dc} \left[1 + \alpha_{dc} \frac{G_{B1}}{G_{Bo}} e^{i\omega t} \right]$$

$$A(t) = A_0 \left[1 + \alpha_{rf} \frac{G_{B1}}{G_{Bo}} e^{i\omega t} \right]$$
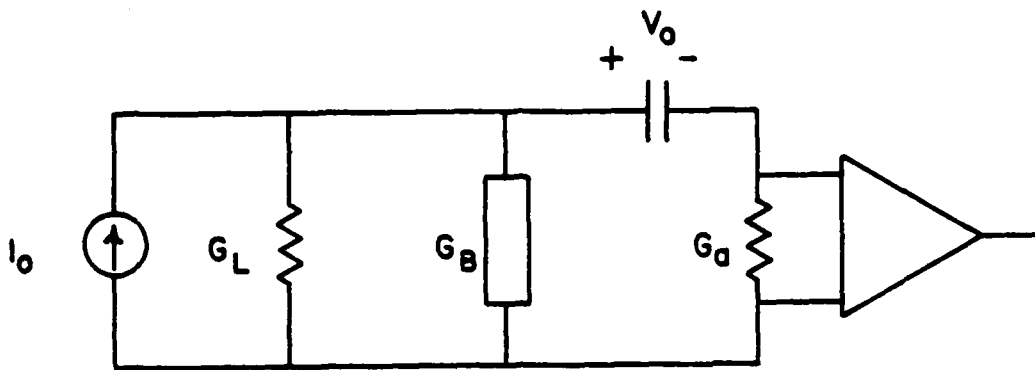
and

4

Fig. 2   Bias and IF circuitry.

$$P(t) = P_{dc} + A_0 P_{rfo} + \left[(\alpha_{dc} P_{dc} + \alpha_{rf} A_0 P_{rfo}) \frac{G_{B1}}{G_{Bo}} + A_0 P_{IF} \right] e^{i\omega t}$$

$$= P_0 + P_1 e^{i\omega t}$$

where

$$P_{dc} = V_B{}^2 G_{Bo} ,$$

$$P_{rfo} = P_{LO} + P_s$$

$$P_{IF} = 2 \left(P_{LO} P_s \right)^{1/2} \text{ (heterodyne detection)}$$

$$= P_s \qquad \text{(direct detection)}$$

$$A_0 = \frac{G_{Bo} Z_0}{(1 + G_{Bo})^2}$$

$$\alpha_{dc} = \frac{G_B}{P_{dc}} \frac{\partial P_{dc}}{\partial G_B} \bigg|_{G_B = G_{Bo}} = \frac{G_a + G_L - G_{Bo}}{G_a + G_L + G_{Bo}}$$

$$\alpha_{rf} = \frac{G_B}{A} \frac{\partial A}{\partial G_B} \bigg|_{G_B = G_{Bo}} = \frac{1 - G_{Bo} Z_0}{1 + G_{Bo} Z_0}$$

At optical frequencies, it is customary to consider the absorption coefficient A as an infrared quantum efficiency η. When the bolometer is matched to the radiation, $\eta = A = 1$ and $\alpha_{rf} = 0$.

When the bolometer conductance G_B is dependent upon the electron temperature T_e via a power law

5

$$G_B \propto T_e{}^n$$

then

$$\left.\frac{dG_B}{G_B}\right|_{G_B=G_{Bo}} = \frac{G_{B1}}{G_{Bo}} = \left.\frac{dT_e}{T_e}\right|_{T_e=T_o} = n\frac{T_1}{T_o}$$

Power loss to the lattice is determined by the equation:

$$C\frac{d}{dt}(T_e-T_L) + K(T_e-T_L) = P(t)$$
$$= P_o + P_1 e^{i\omega t} \quad .$$

Letting the electron temperature have a steady state value T_o and a time dependent part $T_1 e^{i\omega t}$, we obtain two equations for T_o and T_1 whose solutions are:

$$T_o - T_L = \frac{P_o}{K} = \frac{P_{dc} + A_o P_{rfo}}{K}$$

and

$$\frac{T_1}{T_o} = \frac{A_o P_{IF}}{K'T_o(1+i\omega\tau')}$$

in which

$$K'T_o = KT_o - n\left[\alpha_{dc}P_{dc} + \alpha_{rf}A_o P_{rfo}\right]$$

and

$$\tau' = \frac{C}{K'}$$

6

From the expression for T_1/T_0, we can calculate the variation in bolometer conductance at the IF frequency:

$$\frac{G_{B1}}{G_{Bo}} = \frac{nA_oP_{IF}}{K'T_o(1+i\omega\tau')} \quad .$$

From Fig.2, the magnitude of the potential across the IF amplifier is:

$$v_a = \frac{I_o}{G_{Bo}+G_L}\frac{G_{Bo}}{G_a+G_L+G_{Bo}}\frac{G_{B1}}{G_{Bo}}$$

$$= V_{dc}\frac{G_{Bo}}{G_a+G_L+G_{Bo}}\frac{nA_oP_{IF}}{K'T_o\left[1+(\omega\tau')^2\right]^{1/2}}$$

and the amplifier current is:

$$i_a = I_{dc}\frac{G_a}{G_a+G_L+G_{Bo}}\frac{nA_oP_{IF}}{K'T_o\left[1+(\omega\tau')^2\right]^{1/2}} \quad .$$

The rms voltage, rms current, and average power into the amplifier are then given by:

$$v_a = \frac{(P_{dc}G_{Bo})^{1/2}}{2}\frac{nP_{IF}}{KT_o}\frac{1}{(G_a+G_L+G_{Bo}) - (G_a+G_L-G_{Bo})(nP_{dc}/KT_o)}$$

$$i_a = \frac{(P_{dc}G_{Bo})^{1/2}}{2}\frac{nP_{IF}}{KT_o}\frac{G_a}{(G_a+G_L+G_{Bo}) - (G_a+G_L-G_{Bo})(nP_{dc}/KT_o)}$$

$$P_a = \frac{v_ai_a}{2} = \frac{P_{dc}G_{Bo}G_a(nP_{IF}/KT_o)^2}{2[(G_a+G_L+G_{Bo}) - (G_a+G_L-G_{Bo})(nP_{dc}/KT_o)]^2}$$

For the heterodyne case, $P_{IF} = 2 \left(P_{LO}P_s\right)^{1/2}$.

For the direct detection case, $P_{IF} = P_s$.

The bandwidth of the bolometer is given by:

$$B = \frac{1}{2\pi\tau'} = \frac{K'}{2\pi C} = B_0 \left[1 - \frac{nP_{dc}}{KT_0} \frac{G_a + G_L - G_{Bo}}{G_a + G_L + G_{Bo}}\right]$$

where B_0 is the bandwidth when $G_a + G_L = G_{Bo}$.

2. Device Modeling - Noise Analysis

The minimum detectable signal by any receiver is determined by the conversion loss, calculated in the previous section, and the noise sources which give an appreciable contribution at the amplified IF output. Previous investigators have restricted their analysis to the case where amplifier noise is dominant [4,5] or have used restricted circuitry assumptions [1,2,3]. A general noise analysis is presented in this section; noise sources discussed include a) local oscillator shot noise, b) background fluctuations, c) electron temperature fluctuations, d) Johnson-Nyquist noise and e) amplifier noise. Adequate high pass filtering to eliminate 1/f noise will be assumed since frequencies of interest will fall considerably above the knee of typical 1/f curves.

2.1 Local Oscillator Shot Noise

The fundamental noise floor for a heterodyne device with a high quality local oscillator can be no lower than that produced by statistical fluctuations in the local oscillator. This result is independent of detector or system parameters and yields a noise temperature given by

$$T_{nLO} = hf/k_B A_0 \ .$$

8

2.2 Background Noise

Fluctuations in the background seen by a receiving antenna set the theoretical sensitivity limit of the receiving system. The antenna can be characterized by a radiation resistance R_{bg} describing how well the antenna is matched to the transmission line carrying the signal to the receiver, and a temperature T_{bg} describing the effective background or sky temperature. T_{bg} is given by the equation

$$T_{bg} = \frac{1}{4\pi} \int T(\theta,\phi)G(\theta,\phi)d\Omega$$

where $T(\theta,\phi)$ = sky temperature in the incremental solid angle $d\Omega$ in the (θ,ϕ) direction,

$G(\partial,\phi)$ = antenna gain in (θ,ϕ) direction.

For the frequency range of interest for the hot electron bolometer, 90 to 500 GHz, the sky temperature lies between $50^{\circ}K$ at 94 GHz for an antenna pointing away from the earth in clear weather to $290^{\circ}K$ for other frequencies and/or weather conditions and/or directions where the earth's surface is partially subtended.

The transmission line carrying the signal from the antenna to the receiver can be characterized by a loss L, a characteristic impedance Z_0 and a physical temperature T_{TL} (See Fig. 3). For maximum sensitivity, the line is matched to the antenna, i.e., $Z_0 = R_{bg} = R_{bg}'$. The effective background temperature referred to the receiver end of the transmission line is [7]:

$$T_{bg}' = T_{bg}L + T_{TL}(1 - L)$$

where L < 1. As expected, for high loss the noise originates mainly in the transmission line while for small L, background fluctuations dominate.
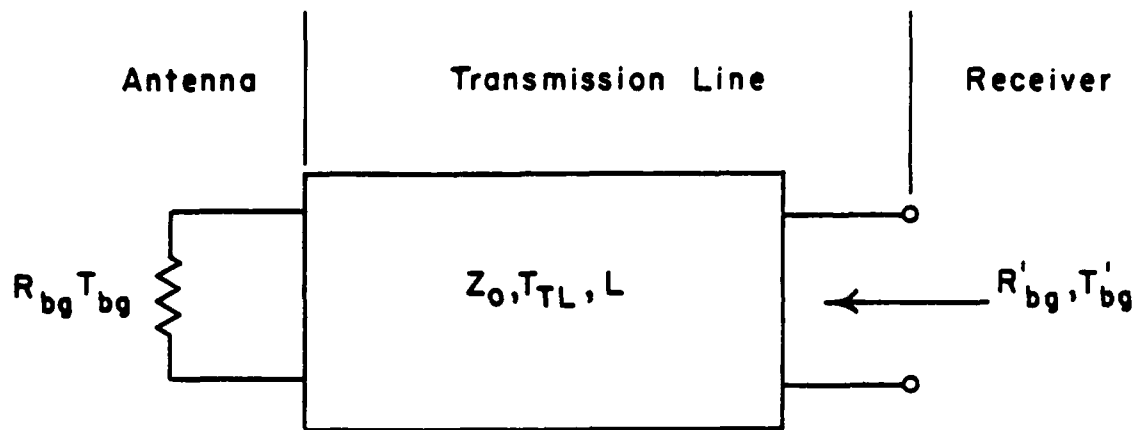
9

Fig. 3   Circuit representation of antenna and transmission line to the receiver.

The background contribution to the noise power can be computed by calculating the noise emanating from a resistor Z_0 at temperature T_{bg}'. The expression for e_{bg}' in Fig. 4 holds in the low frequency limit ($hf \ll k_B T_{bg}'$), easily met in the current case. The previous development for signal power delivered to the amplifier can be used directly to compute the noise originating from from background fluctuations by making the substitution

$$P_s = P_{bg} = \frac{e_{bg}'^2}{4Z_0} k_B T_{bg}' B .$$

2.3 Temperature Fluctuation Noise

The random relaxation of hot electrons to the lattice and subsequent absorption of energy leads to random fluctuations in the electron temperature; i.e., temperature fluctuation noise. For a general heat balance equation of the form

$$C \frac{d}{dt} \Delta T + K' \Delta T = W(t)$$

Van der Ziel [8] shows that temperature fluctuations take the form

$$(\delta T)^2 = \frac{4 k_B T_0^2 B}{K' \left[1 + (\omega \tau')^2\right]} \quad \text{where } \tau' = C/K' .$$

10
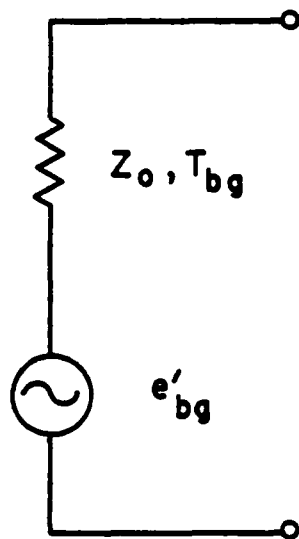
$$e'^2_{bg} = 4K_B T'_{bg} Z_0 B$$

$$B = \text{Receiver Bandwidth}$$

Fig. 4   Equivalent source for background noise.

Fluctuations in temperature are related to fluctuations in conductivity through the expression:

$$\frac{\delta G_{Bo}}{G_{Bo}} = n \frac{\delta T_0}{T_0} \quad ,$$

which in turn is related to fluctuations in power delivered to the amplifier by

$$\delta P_a = \frac{P_{dc}}{2} \frac{G_{Bo} G_a}{(G_{Bo}+G_a+G_L)^2} \frac{(\delta G_{Bo})^2}{G_{Bo}} \quad ,$$

so that

$$P_{nTF} = \frac{2 P_{dc} n^2 k_B T_0 G_{Bo} G_a B}{K' T_0 (G_{Bo}+G_L+G_a)^2} \quad .$$

2.4 Johnson-Nyquist Noise

In the low frequency limit, $hf \ll k_B T$, the noise current originating from a conductance G at temperature T is given by

$$i_{nJ}^2 = 4 k_B T B G \quad .$$

11

Again referring to Fig.2, the total Johnson noise delivered to the amplifier input terminals is

$$P_{nJ} = 4k_B G_a B \; \frac{G_L T_L + G_{Bo} T_o}{(G_L + G_a + G_{Bo})^2}$$

2.5 Amplifier Noise

In a practical receiver, noise generated within the amplifier which follows the detecting/mixing element will be a significant if not the dominant noise contribution. This is especially true of the present device because of its intrinsically high conversion loss $(L_c > 6 \text{ dB})$.

For the purpose of this discussion we will focus on cooled GaAs FET amplifier technology. Since a low temperature bath must be provided for the bolometer/mixer element, little further complication is introduced by cooling the amplifier. Further, since the amplifier is in close proximity to the bolometer element, the attenuation and frequency-dependent loss inherent in the transmission line needed to transport the signal out of the dewar are minimized. These losses can be particularly troublesome at high IF frequencies when the amplifier is not well matched to the bolometer, and as will be shown in the following section, a match between the bolometer and amplifier does not result in the lowest conversion loss. An attractive configuration was introduced by Williams, Lum, and Weinreb [9] for radio astronomy observations. The noise contribution of their FET amplifier is conveniently represented by a noise temperature T_a referred to the amplifier input terminals. The input impedance can be adjusted over a wide range by changing the source inductance of the amplifier circuit without altering the noise temperature. Noise temperatures $\sim 130^\circ\text{K}$ have been reported at 1.3 GHz and no degradation is expected for lower IF frequencies provided that the 1/f region of the spectrum is avoided [10].

12

3. Heterodyne Detection Performance

3.1 Noise temperature for minimum conversion loss

A common way of characterizing heterodyne receiver performance is by means of an effective noise temperature T_{eff}, implying that the minimum detectable signal power is $k_B T_{eff} B$ for a unity signal-to-noise ratio at the receiver output. Since the amplifier noise contribution has been referred to the amplifier input terminals, the effective noise temperature is found by equating the signal at the amplifier input terminals to the sum of all noise contributions at these terminals. Thus, in the low IF frequency limit,

$$T_{eff} = hf/k_B A_o \qquad \text{(local oscillator shot noise)}$$

$$+ \; T_{bg}{}' \qquad \text{(background noise)}$$

$$+ \; \frac{KT_o{}^2}{A_o{}^2 P_{LO}} \qquad \text{(thermal fluctuation noise)}$$

$$+ \; \frac{2K^2 T_o{}^3}{n^2 A_o{}^2 P_{LO} P_{dc}} \left[1 + \frac{G_L}{G_{Bo}} \frac{T_L}{T_o} \right] \qquad \text{(Johnson noise)}$$

$$+ \; T_a L_c \qquad \text{(amplifier noise)},$$

where

$$L_c = \frac{K^2 T_o{}^2}{2 n^2 A_o{}^2 P_{dc} P_{LO}} \frac{(G_a + G_L + G_{Bo})^2}{G_a G_{Bo}}$$

is the conversion loss of the mixer ($L_c > 1$).

We will now minimize T_{eff} by appropriate choice of circuitry and bias parameters. First, it can be seen that it is advantageous to employ a constant current bias ($G_L = 0$) and match the signal input transmission line to

13

the bolometer ($A_0 = 1$). The importance of low conversion loss L_C may be readily appreciated as the noise contribution of the amplifier can be seen to be directly proportional to L_C. However, conversion loss need only be reduced sufficiently to allow the amplifier noise to be suppressed below the other noise sources. Additional decreases in L_C yield no benefit.

It can be noted that both the amplifier contribution to the effective noise temperature, T_{na}, and the Johnson noise have the same functional dependence on P_{LO} and P_{dc}. To minimize these noise contributions we follow the approach of Arams [5] and determine the optimum relationship between P_{dc} and the total power applied $P_0 = P_{LO}+P_{dc}$. The assumption of $P_0 =$ constant implies a fixed electron temperature T_0 and a fixed bolometer conductance G_{Bo}. The optimum value is

$$P_{dc}{}^{opt} = \frac{P_0}{2 - \frac{nP_0}{KT_0}\frac{G_a-G_{Bo}}{G_a+G_{Bo}}}$$

giving a noise contribution of

$$T_{na} = 8\,\frac{KT_0}{nP_0}\,\frac{(G_a+G_{Bo})^2}{4G_aG_{Bo}}\left[1 - \frac{nP_0}{KT_0}\frac{G_a-G_{Bo}}{G_a+G_{Bo}}\right]\,T_a\quad .$$

Now T_{na} is minimized by the correct choice of IF impedance mismatching

$$\left.\frac{G_a}{G_{Bo}}\right|_{opt} = \left(\frac{KT_0+nP_0}{KT_0-nP_0}\right)^{1/2}\quad .$$

Under this assumption

$$T_{na} = 4\left(\frac{KT_0}{nP_0}\right)^2\left[1 + \left[1 - \left(\frac{nP_0}{KT_0}\right)^2\right]^{1/2}\right]\,T_a\quad .$$

14

It can further be shown [5] that $nP_O/KT_O < 1$, so that

$$T_{na}\bigg|_{minimum} = 4T_a,$$

the theoretical limit for resistive mixers. In practice, one does not
operate close to this limit since the bandwidth approaches zero. It should
also be noted that the analysis of Section 1 breaks down in this limit
because the assumption $T_1 \ll T_O$ is no longer fulfilled.

Using the optimized value $P_{dc}{}^{opt}$, the Johnson noise contribution to the
effective noise temperature is:

$$T_{nJ} = 8\left(\frac{KT_O}{nP_O}\right)^2 \left[1 - \left(\frac{nP_O}{KT_O}\right)\left(\frac{G_a - G_{BO}}{G_a + G_{BO}}\right) \right] T_O \ .$$

Unlike the amplifier noise, this quantity is minimized when $G_a \gg G_{BO}$ (i.e.,
for a current amplifier) and becomes small as nP_O/KT_O approaches unity.

Finally, the temperature fluctuation noise can be written

$$T_{nTF} = nT_O \ \frac{1 - \dfrac{nP_O}{KT_O} \dfrac{G_a - G_{BO}}{G_a + G_{BO}} \dfrac{P_{dc}}{P_O}}{\dfrac{nP_O}{KT_O}(1 - P_{dc}/P_O)}$$

The TF noise contribution is generally somewhat smaller than the Johnson or
amplifier noise contributions but it can be seen that $T_{nTF} > T_O$. It reaches
nT_O in the limit $P_{dc}/P_O \to 0$, $nP_O/KT_O \to 1$, a different condition than for the

other noise contributions. Under the amplifier noise optimizing condition, $P_{dc} = P_{dc}{}^{opt}$, it takes the simple form

$$T_{nTF} = 2 \frac{KT_0{}^2}{P_G} \quad .$$

3.2 Bandwidth

The bandwidth must be considered along with the noise temperature in optimizing circuitry for a given application. With $G_L = 0$,

$$B = \frac{1}{2\pi\tau'} = \frac{K'}{2\pi C} = B_0 \left[1 - \frac{nP_{dc}}{KT_0} \frac{G_a - G_{Bo}}{G_a + G_{Bo}} \right] \quad .$$

For the entire range of amplifier mismatch conditions

$$1 - \frac{nP_{dc}}{KT_0} < \frac{B}{B_0} < 1 + \frac{nP_{dc}}{KT_0}$$

and

$$0 < \frac{B}{B_0} < 2 \quad .$$

For the special case $P_{dc} = P_{dc}{}^{opt}$,

$$\frac{B}{B_0} = \frac{1 - \frac{nP_0}{KT_0} \frac{G_a - G_{Bo}}{G_a + G_{Bo}}}{1 - \frac{nP_0}{2KT_0} \frac{G_a - G_{Bo}}{G_a + G_{Bo}}} \quad .$$

Results of noise temperature and bandwidth calculations for an FEB heterodyne receiver are presented in Figures 5 thru 8. Relative values of P_{dc} and P_{LO} are chosen to minimize T_{nA} and T_{nJ}. $T = T_0$ is assumed; other cases are readily inferred from these figures. The following points can be noted:

(a) T_{eff} is a sensitive function of the parameter nP_0/KT_0, being minimized when it approaches 1.

(b) T_{eff} reaches a minimum value in the range $1 < G_a/G_{Bo} < \infty$, approaching the lower limit of G_a/G_{Bo} as $nP_0/KT_0 \to 0$ and approaching the upper limit as $nP_0/KT_0 \to 1$.

(c) Amplifier noise and Johnson noise dominate; temperature fluctuation noise is of less importance.

(d) $B/B_0 > 1$ for $G_a/G_{Bo} < 1$. Departures from unity are greatest for large values of nP_0/KT_0.

(e) Lowest values of noise temperature are achieved only with a severe bandwidth penalty.

3.3 Noise Temperature for IF Match

When the IF amplifier is matched to the bolometer, the bandwidth becomes independent of the total power and of the relative power distribution between dc and LO sources. This match condition is a good compromise in that it preserves bandwidth and allows a nearly optimum noise temperature. For this case, the bandwidth is given by

$$B_0 = K/2\pi C$$

and is determined solely by the material constants. The minimum conversion loss becomes
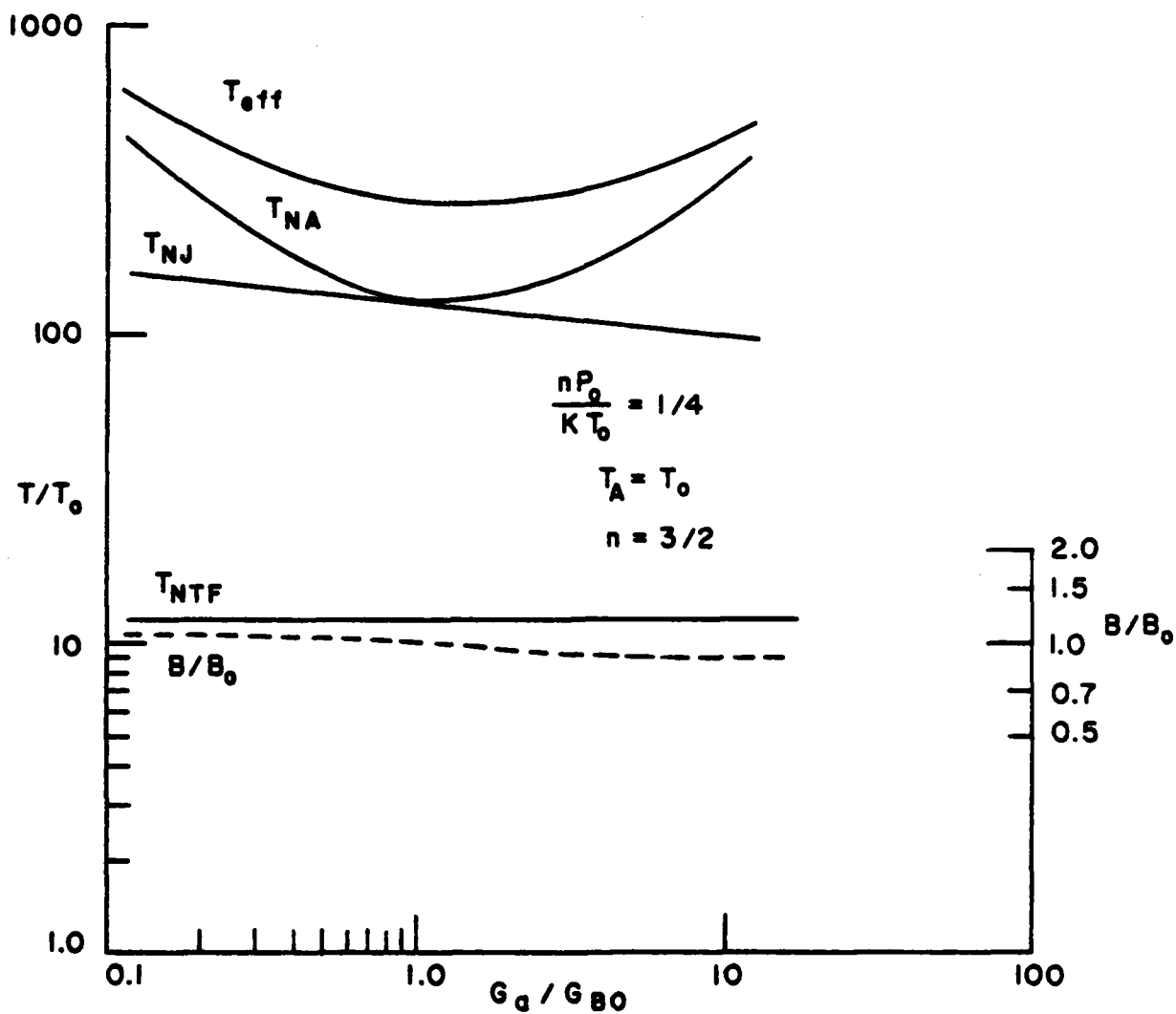
$$L_c = 8(KT_0/nP_0)^2$$

17

Fig. 5   Effective noise temperature as a function of amplifier match for
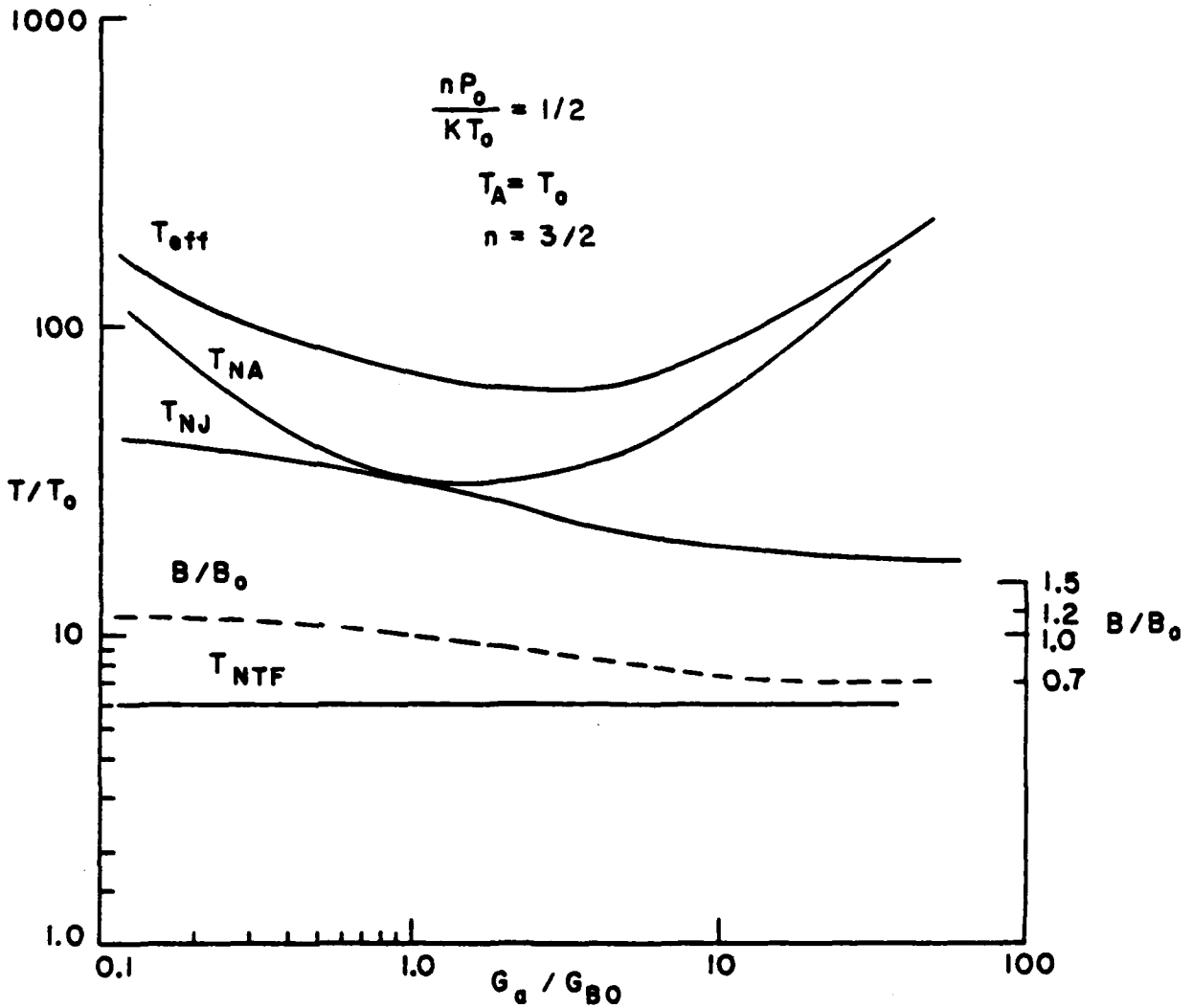$nP_O/KT_O = 1/4$.

Fig. 6   Effective noise temperature as a function of amplifier match for
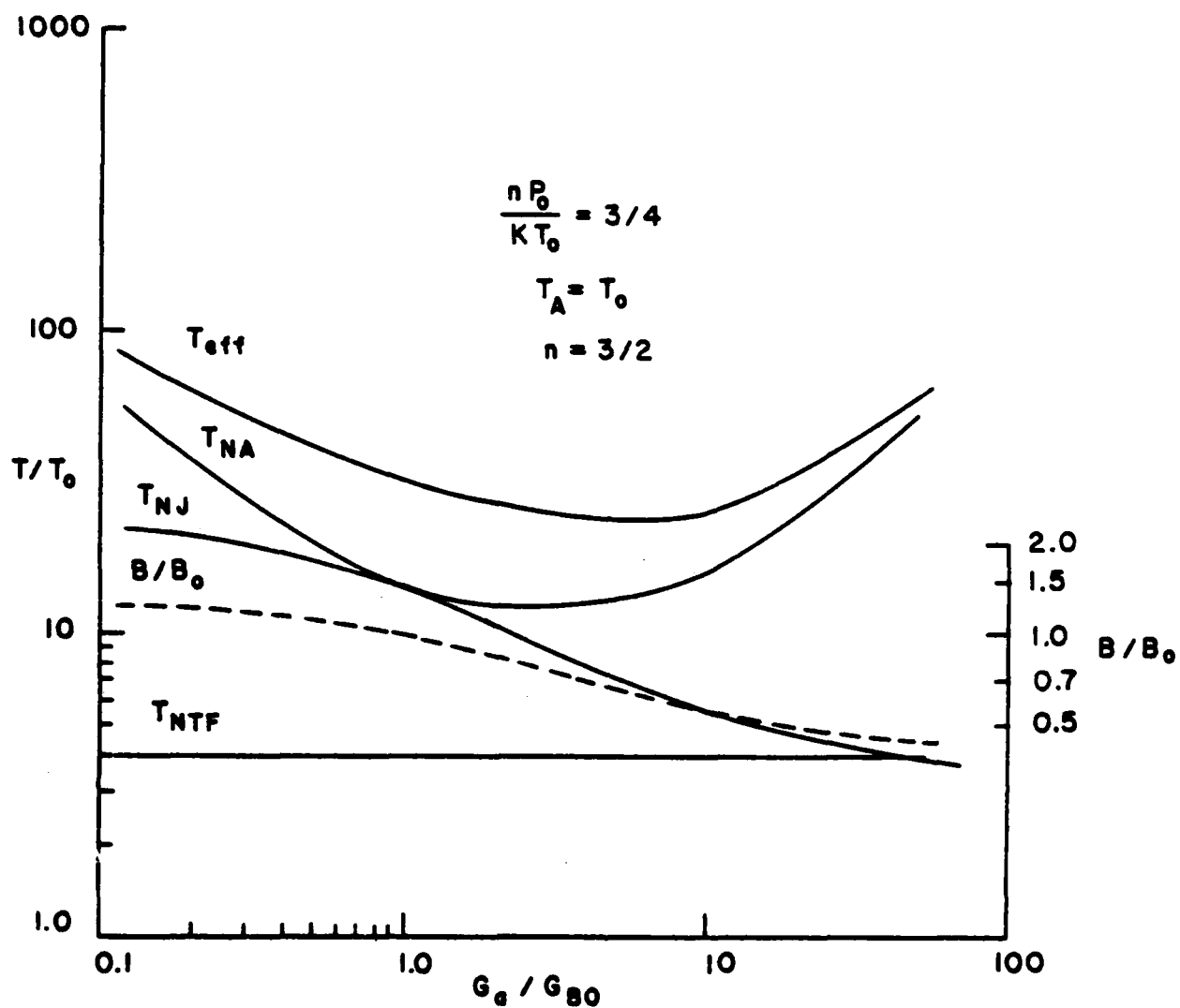 $nP_0/KT_0 = 1/2$.

19

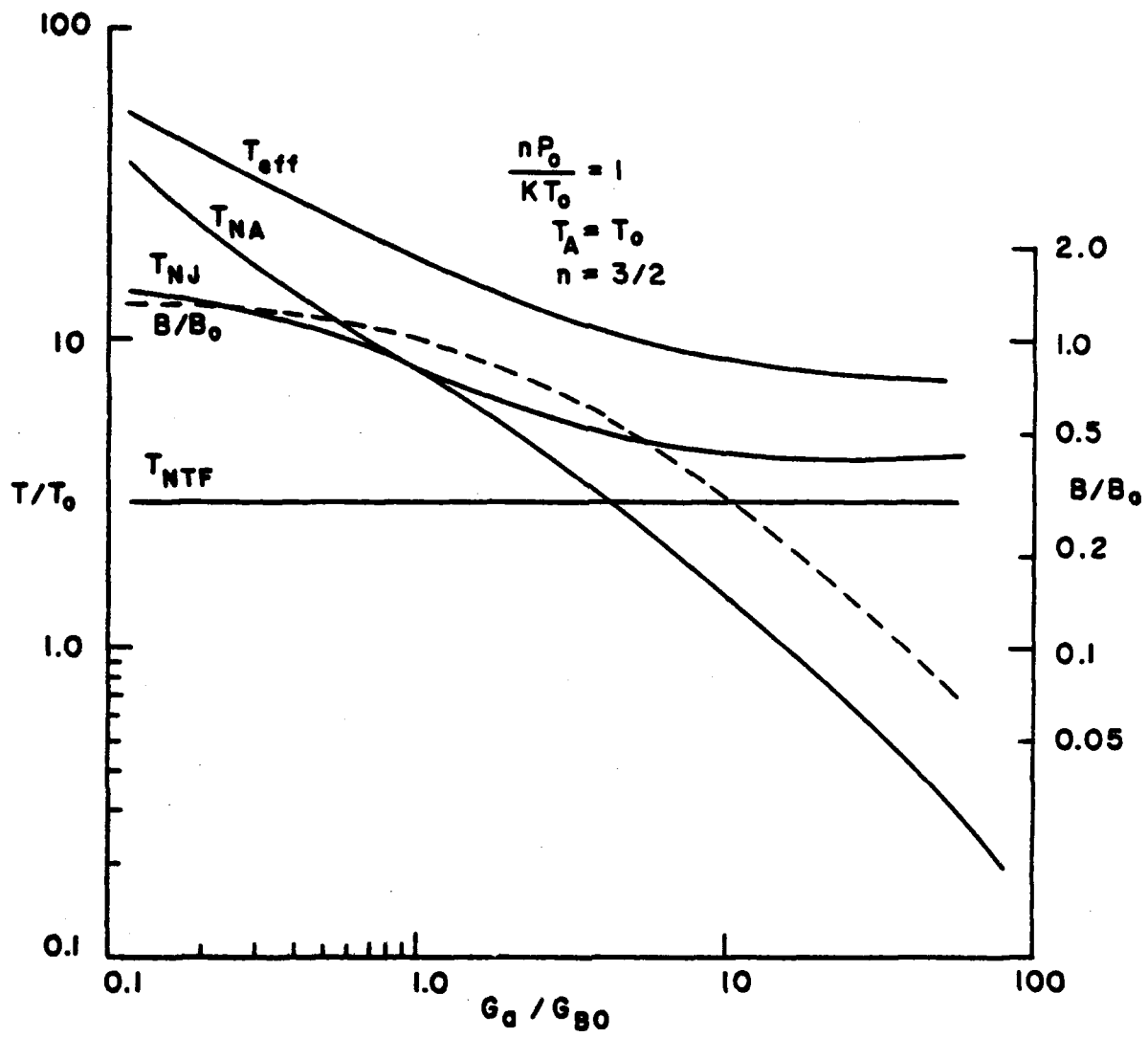Fig. 7   Effective noise temperature as a function of amplifier match for $nP_0/KT_0 = 3/4$.

20

Fig. 8   Effective noise temperature as a function of amplifier match for $nP_0/KT_0 = 1$.

and the total thermal noise contribution (the sum of temperature fluctuation noise and Johnson noise) becomes

$$T_{thermal} = 2KT_O^2/P_O + 8(KT_O/nP_O)^2 T_O \ .$$

Since the steady state electron temperature T_O is related to the lattice temperature T_L by the steady state heat equation

$$KT_O = P_O + KT_L,$$

the total noise temperature may be written

$$T_{eff} = \frac{hf}{k_B} + T_{bg}' + 2\,\frac{KT_L}{P_O}\left(1 + \frac{P_O}{KT_L}\right)^2 T_L + \frac{8}{n^2}\left(\frac{KT_L}{P_O}\right)^2\left(1 + \frac{P_O}{KT_L}\right)^3 T_L$$

$$+ \frac{8}{n^2}\left(1 + \frac{KT_L}{P_O}\right)^2 T_a;$$

where the terms represent quantum, background, thermal fluctuation, Johnson and amplifier noise, respectively.

The thermal contribution and the conversion loss are displayed in Fig. 9 as a function of P_O/KT_L for $n = 3/2$. Optimum performance is achieved for $P_O/KT_L = 2$. When this condition is satisfied the total noise temperature is:

$$T_{eff} = hf/k_B + T_{bg}' + 9T_L + (54/n^2)T_L + (18/n^2)T_a \ .$$

Combining thermal fluctuation and Johnson noise this becomes

$$T_{eff} = hf/k_B + T_{bg}' + 33T_L + 8T_a.$$

This equation expresses the fundamental limit for a free-electron bolometer operating under matched conditions. Material parameters do not appear in this equation and are unimportant as long as the basic conditions are satisfied. These conditions are: (1) the free carriers absorb radiation
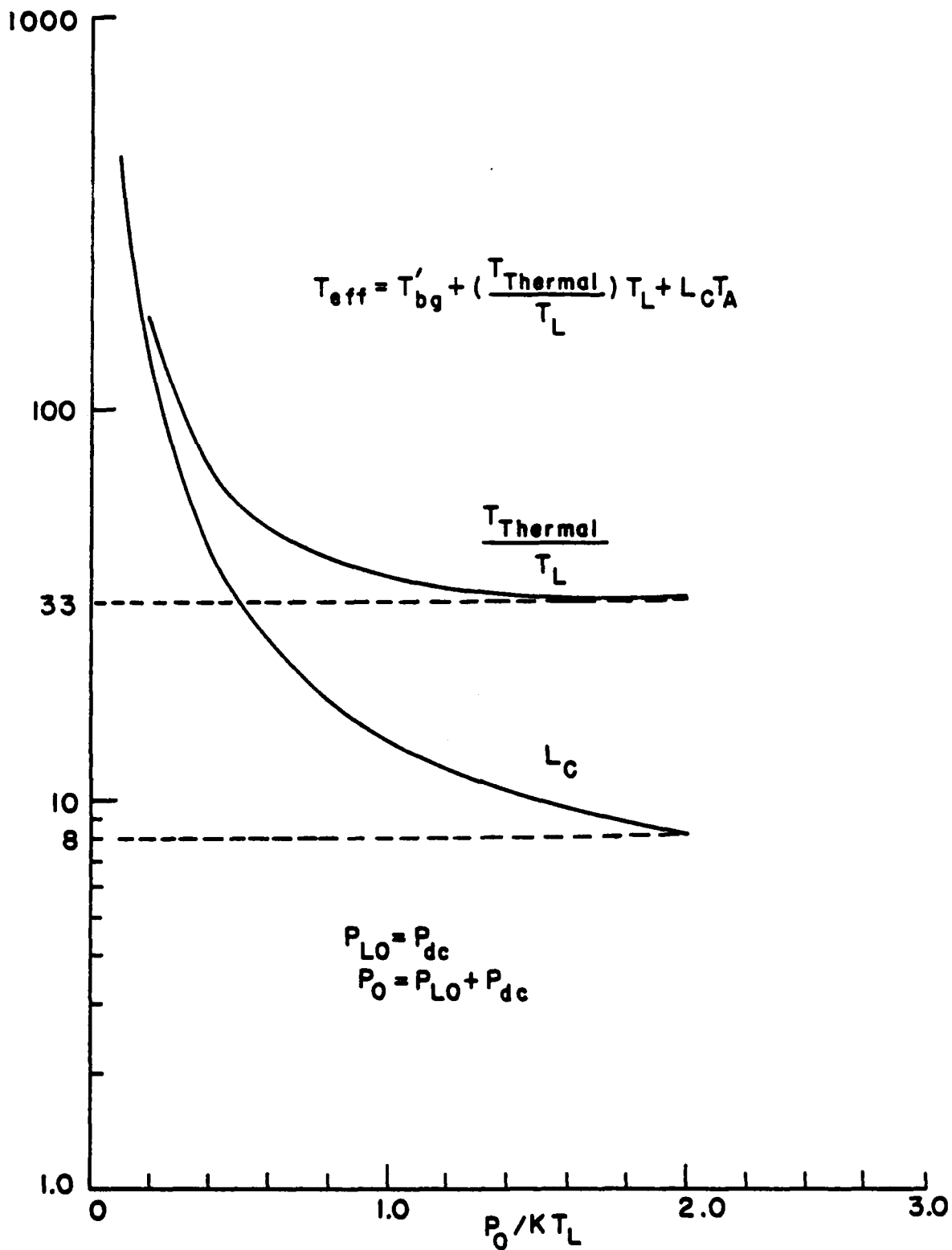
Fig. 9   Effective noise temperature and conversion loss as a function of total power for IF match.

efficiently and (2) ionized impurity scattering dominates the carrier mobility ($n = 3/2$).

It is important to note that the very best performance is only obtained when $P_O/KT_L = 2$ (a condition which is equivalent to $nP_O/KT_O = 1$) and this will be achieved only when the operating point on the IV curve has an infinite slope. If there is a non-infinite thermal conductivity $G_{thermal}$ between the lattice and the sink, then the lattice temperature will be dependent upon the applied power,

$$T_L = T_s \frac{P_O}{1 + G_{thermal} T_s} .$$

For low power, $T_L \simeq T_s$, and the lattice temperature only begins to increase when P_O is of the order of $G_{thermal}T_s$. As T_L begins to rise, K begins to increase very rapidly, especially above 10° K [12]. Thus P_O/KT_L will reach a peak value which is maximized for large values of $G_{thermal}$. This conclusion is consistent with experimental observations by Whalen and Westgate [4] that the maximum achievable value of the parameters nP_O/KT_O decreased significantly as the bath temperature was raised. If the device is to operate with its best noise performance, the lattice should be thermally sunk to the cooled bath through a heat conductance which is as high as possible. If the heat conductance $G_{thermal}$ is infinite, then the lattice temperature is clamped to the sink temperature, K is constant, and P_O/KT_L may be maximized.

4. Direct Detection Performance

The same general approach used above can be employed for direct detection. Here it is more common to express the minimum detectable signal in terms of a noise equivalent power or NEP. The NEP is defined as the signal

applied to the input (antenna) terminals which will lead to a unity signal-to-noise ratio at the receiver output in a 1 Hz bandwidth. Using the results of Section 1 with the substitution $P_{IF} = NEP$, we obtain, assuming $G_L = 0$, $A_O = 1$ and negligible shot noise,

$$NEP^2 = (k_B T_{bg}')^2 + 4k_B T_O K'T_O \left[1 + \frac{2}{n} \frac{K'T_O}{nP_{dc}} + \frac{2}{n} \frac{K'T_a}{nP_{dc}} \frac{(G_a + G_{Bo})^2}{4G_a G_{Bo}} \right]$$

$$\text{where} \quad K'T_O = KT_O \left(1 - \frac{G_a - G_{Bo}}{G_a + G_{Bo}} \frac{nP_{dc}}{KT_O} \right).$$

As in the case of heterodyne detection, the minimum amplifier noise contribution occurs when

$$\frac{G_a}{G_{Bo}} = \frac{KT_O + nP_{dc}}{KT_O - nP_{dc}}$$

implying $G_a > G_{Bo}$. The relative magnitudes of Johnson noise and temperature fluctuation noise are compared with amplifier noise in Figs. 10 to 13. The bandwidth is also shown in the figures. The following points can be observed:

(a) NEP is a sensitive function of nP_{dc}/KT_O being minimized when $nP_{dc}/KT_O \rightarrow 1$.

(b) Amplifier noise and Johnson noise tend to dominate although temperature fluctuation noise becomes appreciable at the higher values of nP_{dc}/KT_O.

(c) NEP is minimum at a slightly higher value of G_a/G_{Bo} than in the heterodyne case.

(d) The bandwidth behavior is similar to that of the heterodyne case: large bandwidth is obtained only at the expense of sensitivity.
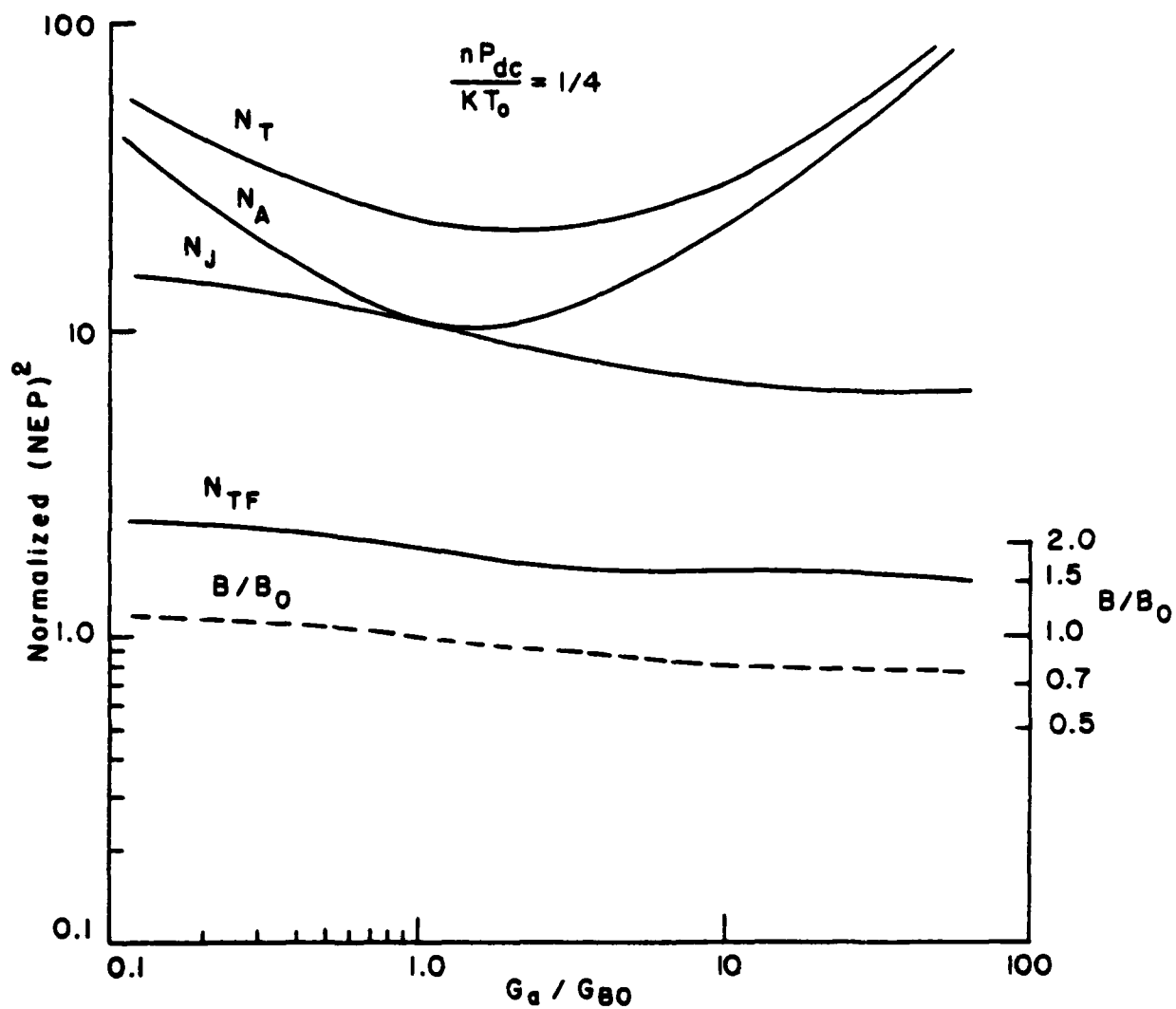
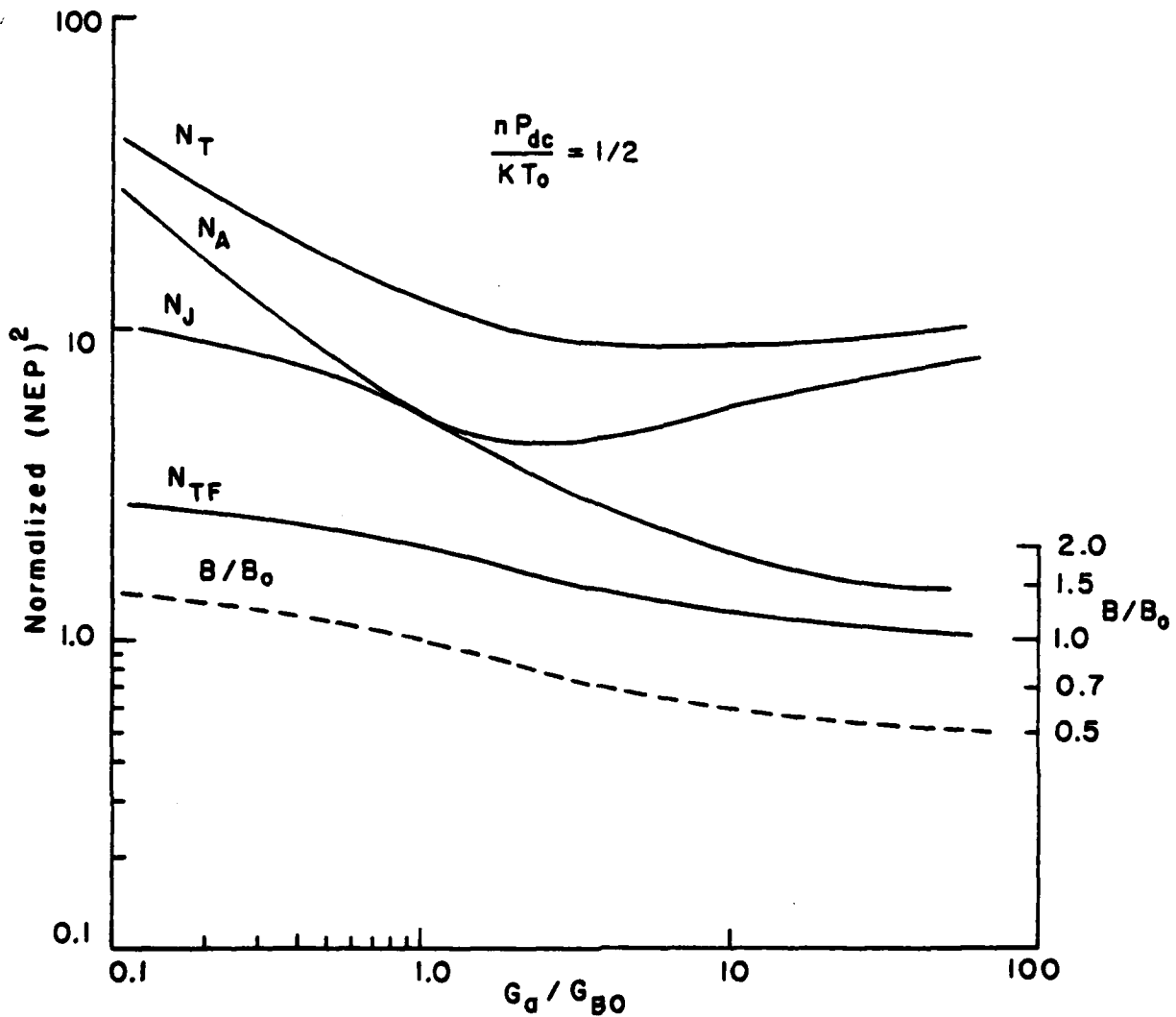Fig.10 $(NEP)^2$ (excluding background noise) normalized to $(4k_BT_0)(K'T_0)$ for $nP_0/KT_0 = 1/4$.

Fig. 11 $(NEP)^2$ (excluding background noise) normalized to $(4k_BT_0)(K'T_0)$ for $nP_0/KT_0 = 1/2$.
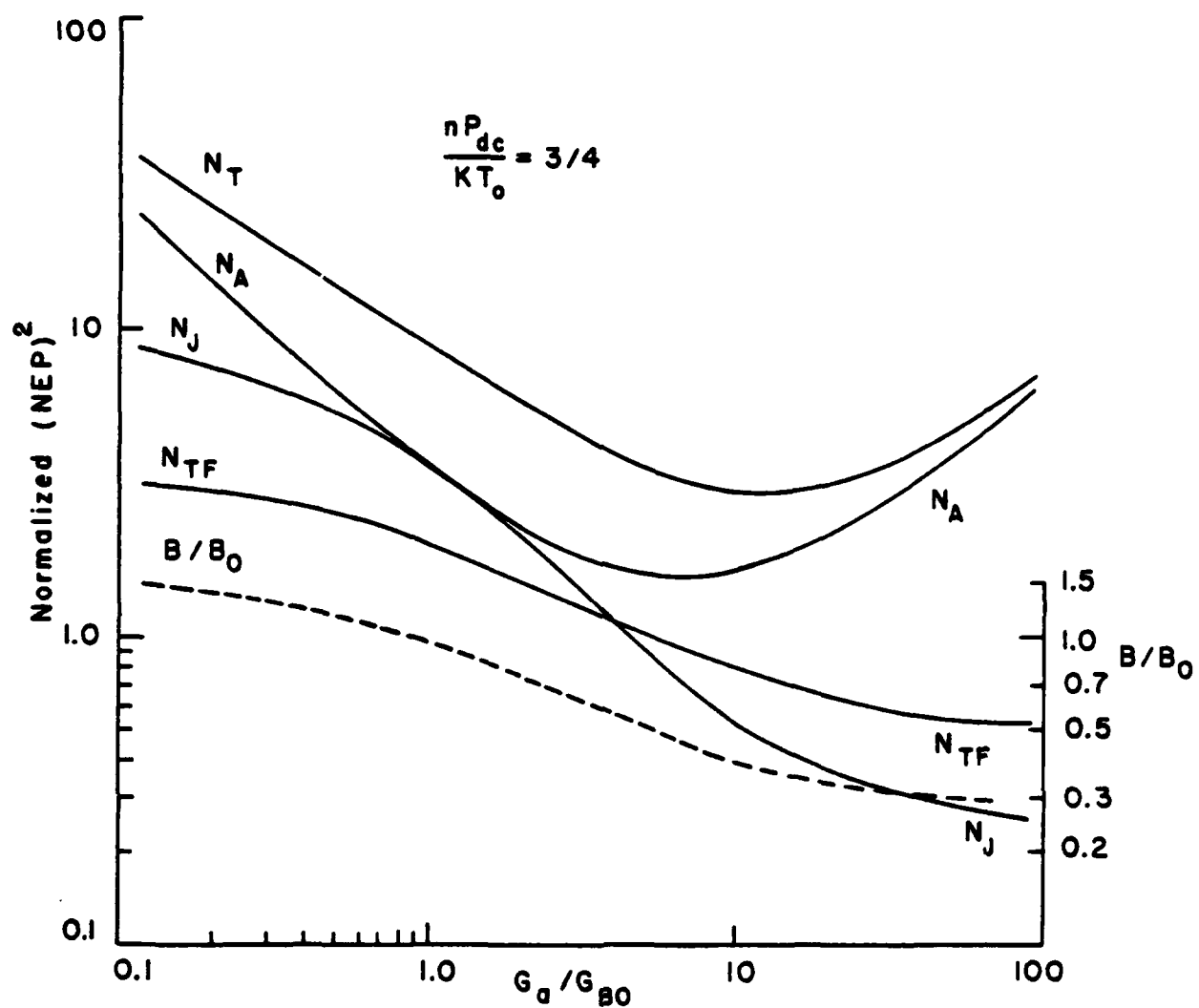
Fig. 12 $(NEP)^2$ (excluding background noise) noramlized to $(4k_BT_o)(K'T_o)$ for $nP_o/KT_o = 3/4$.
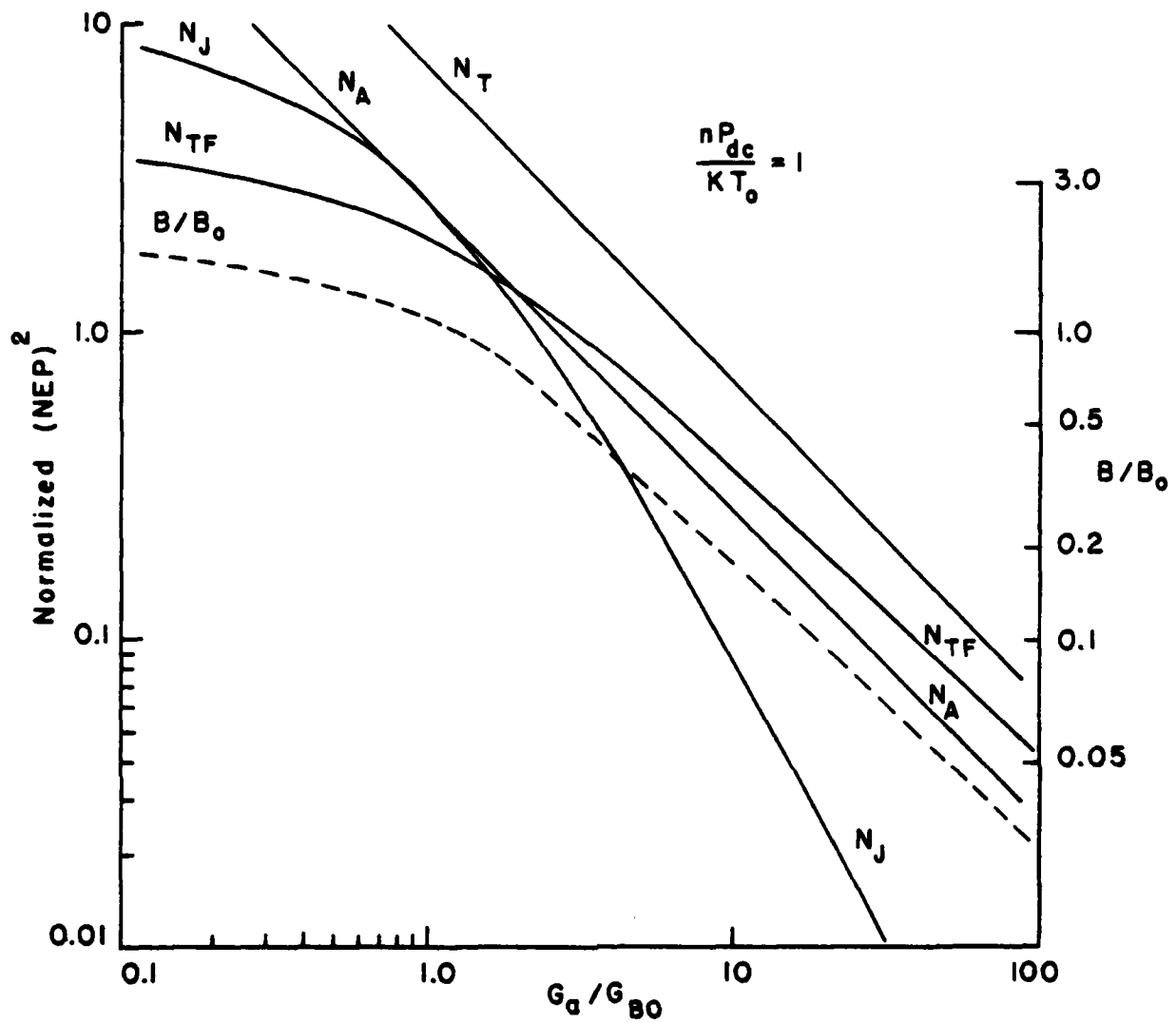
Fig. 13 $(\text{NEP})^2$ (excluding background noise) normalized to $(4k_BT_o)(K'T_o)$ for $nP_o/KT_o = 1$.

5. Conclusion

We have derived a set of equations which describe the performance of free-electron bolometers with all the significant device characteristics included and have given examples of optimization of bias circuit characteristics and local oscillator power.

An ideal free-electron bolometer is shown to have a noise temperature which is limited by the lattice temperature and the noise temperature of the amplifier. Better amplifiers and lower operating temperature yield imnproved performance.

Experimental results from the literature are in good agreement with the calculated maximum performance. With amplifier noise subtracted, the residual detector noise temperature was found [3] to be 150 K. This is in good agreement with the calculated 139 K for a mixer operating at 4.2 K.

These results demonstrate that a severe penalty is paid for increasing device response speed by increasing the operating temperature. A better solution for high speed applications would be selection of a material in which the natural electron-lattice coupling is stronger, resulting in a correspondingly decreased energy relaxation time and faster operation at low temperature. Germanium is an example of a material which may be useful at high speed ($\tau \sim 10^{-9}$ sec). Silicon would be even faster ($\tau \sim 10^{-10}$ sec at 4.2 K). These materials have unfortunately not been sufficiently well characterized to predict their performance as hot electron bolomecers. Fundamental questions such as the magnitude and temperature dependence of the electron-lattice coupling, the saturation behavior or, in fact, if the free electron bolometer effect even exists for useful material compositions have not been resolved.

30

The results in this report do, however, demonstrate that there are no fundamental barriers to achieving low noise temperatures and response times of the order of 10^{-9} sec with free-electron bolometers. Studies of materials other than the usual indium antimonide may allow development of rugged, sensitive, fast broadband heterodyne devices for 100 GHz operation.

References

1. E.H.Putley, Appl.Opt.4, 649 (1965).

2. M.Kinch and B.V.Rollin, Brit.J.Appl.Phys.14, 672 (1963).

3. T.G.Phillips and K.B.Jefferts, Rev.Sci.Instrum.44, 1009 (1973).

4. J.J.Whalen and C.R.Westgate, IEEE Trans.E.D.-17, 310 (1970).

5. F.Arams, C.Allen, B.Peyton, and E.Sard, Proc.IEEE 54, 612 (1966).

6. A.N.Vystavkin and V.N.Gubankov, Sov.Phys.-Semiconductors 2, 968 (1969).

7. W.W.Mumford and E.H.Scheibe, Noise Performance Factors in Communication Systems (Horizon House - Microwave, Inc., Dedham, MA, 1968), p.19.

8. A.Van der Ziel, Noise (Prentice-Hall, Inc., New York, NY, 1954), p.331.

9. D.R.Williams, W.Lum, and S.Weinreb, Microwave Journal, 23, 73 (1980).

10. A.Kerr, private communication.

11. J.J.Whalen, Ph.D thesis, Johns Hopkin University, Baltimore, MD, 1969.

12. M.Kinch, Proc.Phys.Soc.(London), 90, 819 (1967).

END

FILMED

11-83

DTIC